OPEN

Injectable Allograft Adipose Matrix Supports Adipogenic Tissue Remodeling in the Nude Mouse and Human

Lauren E. Kokai, Ph.D.
Benjamin K. Schilling, M.S.
Evangelia Chnari, Ph.D.
Yen-Chen Huang, Ph.D.
Emily A. Imming, B.S.
Arivarasan Karunamurthy, M.D.
Roger K. Khouri, M.D.
Richard A. D'Amico, M.D.
Sydney R. Coleman, M.D.
Kacey G. Marra, Ph.D.
J. Peter Rubin, M.D.

Pittsburgh, Pa.; Edison, N.J.; Miami and Key Biscayne, Fla.; and New York, N.Y.

Background: Adipose tissue reaches cellular stasis after puberty, leaving adipocytes unable to significantly expand or renew under normal physiologic conditions. This is problematic in progressive lipodystrophies, in instances of scarring, and in soft-tissue damage resulting from lumpectomy and traumatic deformities, because adipose tissue will not self-renew once damaged. This yields significant clinical necessity for an off-the-shelf de novo soft-tissue replacement mechanism.
Methods: A process comprising separate steps of removing lipid and cellular materials from adipose tissue has been developed, creating an ambient temperature-stable allograft adipose matrix. Growth factors and matrix proteins relevant to angiogenesis and adipogenesis were identified by enzyme-linked immunosorbent assay and immunohistochemistry, and subcutaneous soft-tissue integration of the allograft adipose matrix was investigated in vivo in both the athymic mouse and the dorsum of the human wrist.
Results: Allograft adipose matrix maintained structural components and endogenous growth factors. In vitro, adipose-derived stem cells cultured on allograft adipose matrix underwent adipogenesis in the absence of media-based cues. In vivo, animal modeling showed vasculature formation followed by perilipin A–positive tissue segments. Allograft adipose matrix maintained soft-tissue volume in the dorsal wrist in a 4-month investigation with no severe adverse events, becoming palpably consistent with subcutaneous adipose.
Conclusions: Subcutaneous implantation of allograft adipose matrix laden with retained angiogenic and adipogenic factors served as an inductive scaffold for sustaining adipogenesis. Tissue incorporation assessed histologically from both the subcutaneous injection site of the athymic nude mouse over 6 months and human dorsal wrist presented adipocyte morphology residing within the injected scaffold. (*Plast. Reconstr. Surg.* 143: 299e, 2019.)

From the Department of Plastic Surgery, School of Medicine, McGowan Institute of Regenerative Medicine, and Department of Bioengineering, University of Pittsburgh; the Departments of Pathology and Dermatology, University of Pittsburgh Medical Center; the Musculoskeletal Transplant Foundation; Florida International University; Miami Breast Center; the Department of Plastic Surgery, Mount Sinai School of Medicine; The Hansjorg Wyss Department of Plastic Surgery, School of Medicine, New York University; and TriBeCa Plastic Surgery.
Received for publication February 19, 2018; accepted July 20, 2018.
This trial is registered under the name "Allograft Adipose Matrix (AAM) in Subcutaneous Dorsal Wrist," ClinicalTrials.gov identification number NCT02445118 (https://clinicaltrials.gov/ct2/show/NCT02445118).
The first two authors contributed equally to this work.

DOI: 10.1097/PRS.0000000000005269

Current nonregenerative therapies for soft-tissue reconstruction are often used in plastic surgery and include biodegradable polymer-based fillers composed of cross-linked hyaluronic acid or poly-L-lactic acid.[1] Despite their

Disclosure: *Dr. Chnari, Dr. Huang, and E. Imming are employees of MTF. Drs. D'Amico, Khouri, and Coleman are paid consultants for MTF. All other authors have no financial interest to disclose. Research was financially supported through a sponsored research agreement between MTF and the University of Pittsburgh. No funding was received for this article.*

biocompatibility and predictability, they fail to provide a regenerative framework necessary for functional improvement, limiting sustained efficacy.[2] Autologous fat transfer has been used widely for correcting soft-tissue defects and contouring irregularities but is plagued by unpredictable outcomes where graft retention can range from 25 to 80 percent relative to the initial volume.[3,4]

Extracellular matrix–based scaffolds have been developed from a variety of tissues, including porcine dermis[5] or urinary bladder,[6] and human dermis,[7] and have shown exceptional clinical promise as regenerative scaffolds. Previous analysis of porcine dermal extracellular matrix scaffolds have shown that the matrix is composed primarily of structural proteins such as collagen and elastin fibrils and glycosaminoglycans, proteins that are known to promote cellular attachment,[8] proliferation, and matrix reorganization.[9] Furthermore, endogenous growth factors such as basic fibroblast growth factor and transforming growth factor-β1 that are typically found within native tissue matrices were preserved after decellularization of porcine dermis. When seeded with adipose-derived stem cells, dermal matrices induced cell differentiation toward an endothelial phenotype, exemplifying that intrinsic structural and instructive properties of the original tissue type remain in the acellular matrix.[10] Previous work with matrices derived from adipose tissue have shown unique protein profiles compared with bladder or dermal matrices and have supported adipogenesis in animal models, but have relied on seeding matrices with adipose-derived stem cells, which was implicated as the adipogenic mechanism.[11–13] Whether a matrix alone can support adipoinduction has yet to be demonstrated in both preclinical and clinical models.

Multiple methods of decellularizing adipose tissue have been addressed in the literature; however, most reports indicate that inclusion of adipose-derived stem cells is necessary for adipose tissue development in vivo.[14–18] We hypothesize that the adipose tissue processing method used here, capable of endogenous angiogenic and adipoinductive factor retention, will create an acellular adipose matrix that is able to promote and sustain adipogenesis in situ without addition of exogenous cells or growth factors.

Supplemental digital content is available for this article. Direct URL citations appear in the text; simply type the URL address into any Web browser to access this content. Clickable links to the material are provided in the HTML text of this article on the *Journal*'s website (www.PRSJournal.com).

MATERIALS AND METHODS

Production of Allograft Adipose Matrix

Allograft adipose matrix was derived from cadaveric human adipose recovered and screened according to American Association of Tissue Banks and U.S. Food and Drug Administration regulations and guidelines, and processed aseptically (Musculoskeletal Transplant Foundation, Edison, N.J.). Lipid was removed by means of exposure to 1-propanol (30 minutes); removal of cellular materials was performed using aqueous sodium deoxycholate under agitation (24 hours); allograft adipose matrix was disinfected using a peracetic acid–based solution (2 hours) and was dehydrated and milled, creating a room temperature–stable allograft. Allograft adipose matrix was distributed in its dehydrated form and reconstituted with saline immediately before use.

Investigation of Matrix-Based Proteins in Native Adipose Tissue and Allograft Adipose Matrix

Antigen retrieval was performed on paraffin-embedded allograft adipose matrix with 10 mM sodium citrate buffer. Primary collagen I, III, IV, and VI antibodies (Abcam, Cambridge, Mass.) were used with hematoxylin counterstain (Sigma-Aldrich, St. Louis, Mo.). Growth factors were extracted using 4 M guanidine hydrochloride in 0.05 M Trizma (Sigma-Aldrich) or T-PER (Thermo Fisher, Waltham, Mass.) over 48 hours at 4°C. Growth factors were quantified using Luminex multiplexing (MilliporeSigma, St. Louis, Mo.) or by enzyme-linked immunosorbent assay (R&D Systems, Minneapolis, Minn.).

In Vitro Characterization of Allograft Adipose Matrix: Cell-Matrix Interactions

Human adipose-derived stem cells recovered from the lipoaspirate of one patient at the Adipose Stem Cell Research Laboratory (University of Pittsburgh, Pittsburgh, Pa.) were expanded in MesenPRO RS (Thermo Fisher) growth medium (37°C, 5% carbon dioxide) until 85 percent confluence was obtained. Allograft adipose matrix, reconstituted in basal medium and Dulbecco's Modified Eagle Medium (Sigma-Aldrich) at 25 percent weight/volume, was placed into 24-well

transwell culture inserts in a 3-mm layer. Human adipose-derived stem cells were seeded atop the matrix, 0.2 M cells per 7-mm diameter. Confocal microscopy was performed using a Leica TCS SPII microscope (Leica, Allendale, N.J.). Fixed human adipose-derived stem cell–seeded allograft adipose matrix was stained with Phalloidin 633 and 4′,6-diamidino-2-phenylindole (all from Thermo Fisher), to visualize attachment and stretching at day 3. Lipid content was visualized by boron-dipyrromethene (Thermo Fisher), at days 7, 14, and 21 after cell seeding. Scanning electron microscopy was performed using FEI XL30 FEG-SEM (FEI, Hillsboro, Ore.) at 5-kV accelerating voltage on days 0, 7, and 14. Immunohistochemistry against collagen VI, collagen IV, and laminin and the adipogenic markers adiponectin, leptin, and FABP4 was performed at days 0, 7, and 14. Imaging was performed using an Olympus IX71 microscope (Olympus, Center Valley, Pa.).

Evaluation of Allograft Adipose Matrix in an Immunocompromised Mouse Model

Allograft adipose matrix was reconstituted in sterile saline and injected bilaterally using a fanning technique in the subcutaneous dorsal flank of 5- to 7-week-old female Nu/Nu mice using a 16-gauge blunt-tip cannula, 0.3 cc per side. Adherence to the regulations and standards set forth by the University of Pittsburgh and the National Institutes of Health Office of Animal Care and Use were strictly followed throughout. Histologic analysis with Masson trichrome and perilipin A immunohistochemistry was performed at each study time point, 3, 6, 12, 18, and 24 weeks, with explants ($n = 5$).

Clinical Evaluation of Allograft Adipose Matrix in the Dorsal Wrist

The prospective pilot clinical assessment, approved by the Institutional Review Board of Concordia Clinical Research (Cedar Knolls, N.J.), investigated allograft adipose matrix injection into the subcutaneous wrist dorsum over a 16-week period. A total of 15 patients were enrolled after informed consent and approval over two sites (TriBeCa Plastic Surgery, New York, N.Y.; and Miami Hand Center, Key Biscayne, Fla.). Inclusion criteria included nonsmoking women aged 35 to 75 years, with a body mass index less than 30 kg/m^2, and with well-controlled blood pressure; exclusions consisted of active infection, collagen disorders, vascular diseases, and deep chemical peels or light/energy-based procedures to the dorsum of the hands within the past year. Allograft adipose matrix was reconstituted using sterile saline immediately before injection according to product instruction, aliquoted into 1-cc syringes, and injected into a 1 × 5-cm site using a 19-gauge blunt-tip cannula in a fanning/tunneling manner incorporating multiple passes after administration of lidocaine 0.5% and epinephrine 1:200,000. Each patient received 2.5 to 5.5 cc of allograft adipose matrix, creating a wheal raised 2 to 3 mm. Patients were followed for 16 weeks with intermittent observation and analysis. The dominant wrist served as a control, not receiving injection. A 2-mm wrist biopsy specimen was recovered from one patient 16 months after injection. Biopsy histology included hematoxylin and eosin and staining against perilipin A (Abcam), developed with 3,3′-diaminobenzidine chromogen. Evaluation was performed by a board-certified pathologist. Statistical analysis was performed in Minitab 17 (Minitab, Inc., State College, Pa.) using the t test, where a value of $p < 0.05$ was considered significant.

RESULTS

Allograft Adipose Matrix Retains Membrane Proteins and Growth Factors

Essential collagens were verified in allograft adipose matrix by immunohistochemical staining. The basement membrane constituent, collagen IV, fibril-forming collagens I and III, and the microfibrillar collagen VI were confirmed in native subcutaneous adipose before allograft adipose matrix creation, and again on completion of the process. (**See Figure, Supplemental Digital Content 1**, which shows immunohistochemistry of collagens VI, IV, III, and I in native adipose tissue and confirmed for retention in allograft adipose matrix after all processing was completed. *Scale bars* = 500 μm. The intended purpose was to provide evidence that key adipose tissue collagens are retained through the allograft adipose matrix process, ***http://links.lww.com/PRS/D240***.) Growth factor quantification verified the presence of various angiogenic and adipogenic proteins. [**See Table, Supplemental Digital Content 2**, which shows the quantified growth factors present in native adipose and their relative quantities after the allograft adipose matrix process (+, increased concentration within an order of magnitude; ++, increased concentration beyond an order of magnitude; o, absence of factor). The intended purpose was to provide evidence that key adipose tissue growth factors are retained through the allograft adipose matrix process. *AAM*, allograft adipose matrix, ***http://links.lww.com/PRS/D241***.]

Human Adipose-Derived Stem Cells Undergo Adipogenesis When Cultured on Allograft Adipose Matrix Scaffolds

Confocal imaging demonstrated that calcein AM–stained human adipose-derived stem cells attached and infiltrated allograft adipose matrix (Fig. 1, *above*, *left*), further supported by fluorescein phalloidin–labeled cytoskeletal actin (Fig. 1, *above*, *right*). In media without adipogenic supplements, human adipose-derived stem cells produced new matrix as early as day 7 (Fig. 1, *below*, *left*), where adipocyte morphology became increasingly pronounced by day 14. [**See Figure, Supplemental Digital Content 3**, which shows (*above* and *center*) scanning electron microscopic images of allograft adipose matrix (*AAM*) alone, allograft adipose matrix seeded with adipose-derived stem cells (*ASCs*) for 7 days, and allograft adipose matrix seeded with adipose-derived stem cells for 14 days cultured in basal medium. (*Below*) Confocal imaging of adipose-derived stem cell–seeded matrices demonstrated increasing lipid content (boron-dipyrromethene, *green*) after exposure to allograft adipose matrix up to day 21 (original magnification, × 20). The intended purpose was to provide a broader scanning electron

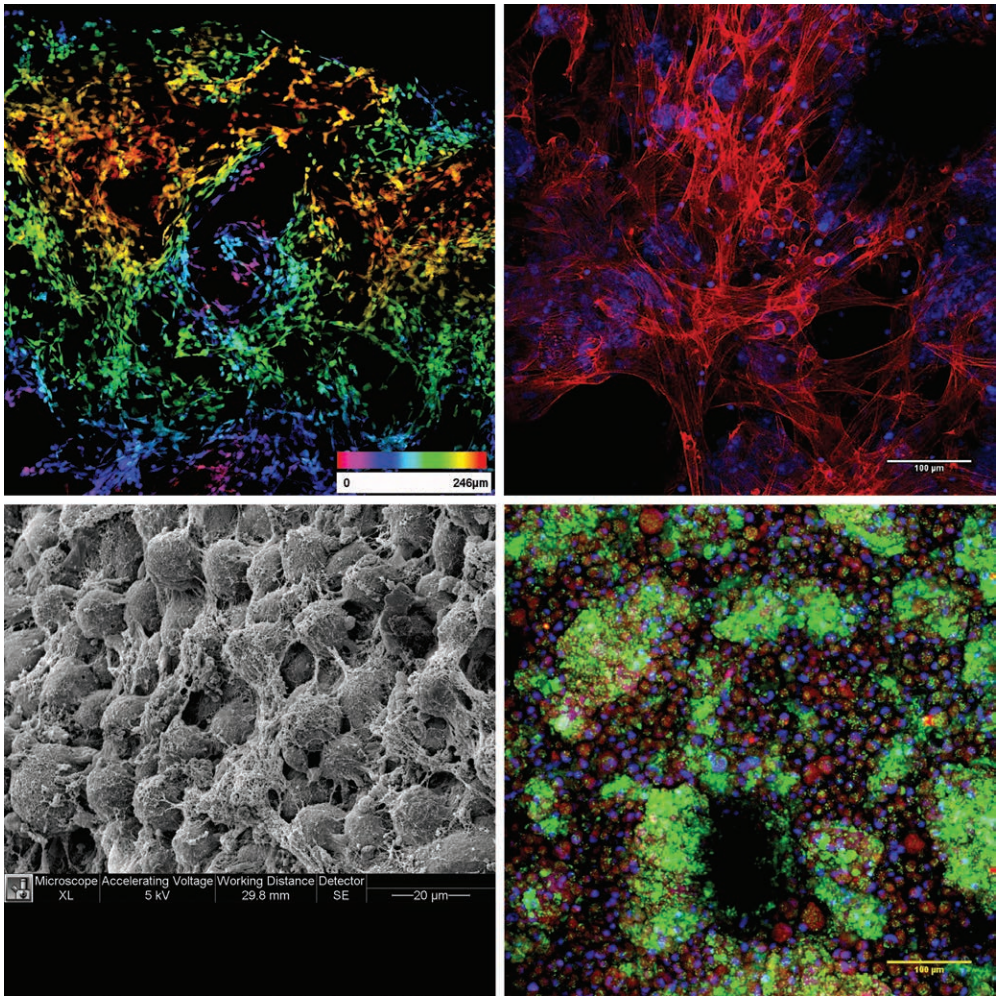

Fig. 1. Human adipose-derived stem cells proliferate on allograft adipose matrix. (*Above*, *left*) Confocal micrograph of human adipose-derived stem cells stained with calcein AM on allograft adipose matrix, with colors corresponding to the depth of infiltrating cells from the surface of the tissue, up to 246 µm. (*Above*, *right*) Adipose-derived stem cell–seeded matrix at day 3 after seeding visualized for cell adhesion marker, actin (fluorescein phalloidin, *red*) and 4′,6-diamidino-2-phenylindole stain for DNA (*blue*). (*Below*, *left*) Scanning electron microscopic image of allograft adipose matrix seeded with adipose-derived stem cells for 7 days, cultured in basal medium. (*Below*, *right*) Confocal imaging of adipose-derived stem cell–seeded matrices demonstrating lipid content (boron-dipyrromethene, *green*) after exposure to allograft adipose matrix at day 7 (original magnification, × 20).

microscopic and boron-dipyrromethene imagery time course, expanding on data shown (Fig. 1), ***http://links.lww.com/PRS/D242***.] Lipid was visualized using fluorescent boron-dipyrromethene, which showed intracellular lipid accumulation within the first 7 days of culture on allograft adipose matrix (Fig. 1, *below*, *right*). Immunohistochemical analysis revealed that human adipose-derived stem cells secreted matrix proteins and adipogenic markers. [**See Figure, Supplemental Digital Content 4**, which shows that allograft adipose matrix (*AAM*) supports in vitro adipogenesis of human adipose-derived stem cells (*ASCs*) seeded onto the matrix. Immunohistochemical staining of allograft adipose matrix alone, allograft adipose matrix seeded with adipose-derived stem cells for 7 days, and allograft adipose matrix seeded with adipose-derived stem cells for 14 days of culture in basal medium. *Scale bar* = 50 μm for all images. The intended purpose was to display the inherent adipogenic capabilities of the allograft adipose matrix material using adipose-derived stem cells cultured onto the matrix without differentiation-inducing media, ***http://links.lww.com/PRS/D243***.]

Allograft Adipose Matrix Implantation in Athymic Mice Supports Adipogenesis In Situ

Bilateral injections of allograft adipose matrix in the immunocompromised mouse dorsal flank was used as the preclinical model, consistent with previous literature.[19–23] Here, 0.3 cc of saline-reconstituted allograft adipose matrix was injected diffusely through a 16-gauge blunt-tip cannula bilaterally (Fig. 2, *above*). Grafted material was excised at 3, 6, 12, 18, and 24 weeks and examined grossly for texture and pliability. Tissue architecture remodeling was examined with Masson trichrome staining, and adipocyte presence were confirmed by means of perilipin A

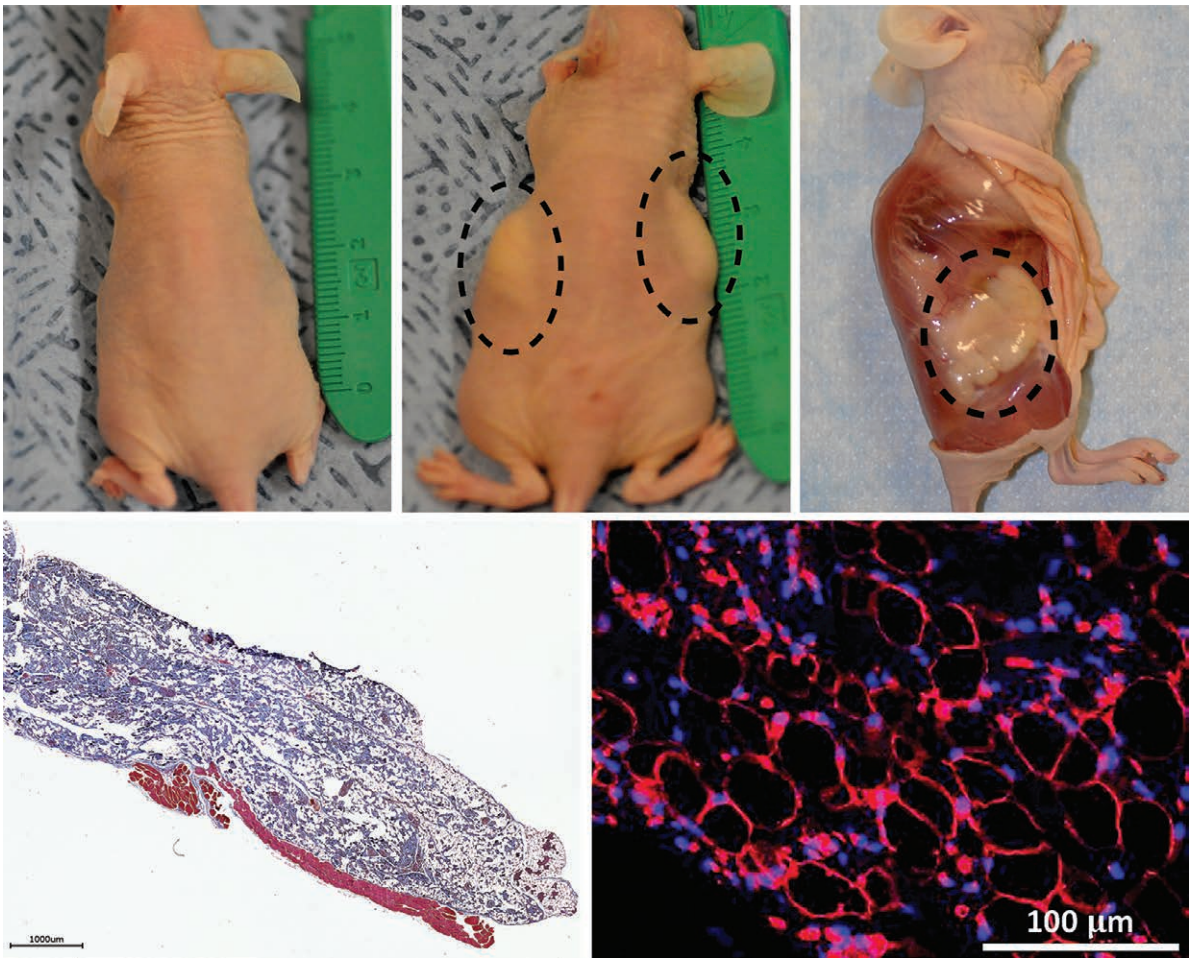

Fig. 2. (*Above*) Acellular adipose matrix was implanted into immunocompromised mice on the dorsal flank as bilateral 0.3-ml diffuse injections, where *dashed ellipses* identify the location of the injections. (*Below*) Masson trichrome showed the presence of adipocytes within material at week 24, confirmed by perilipin A immunofluorescence.

immunofluorescence (Fig. 2, *below*). No adverse events were observed throughout the murine study. Inflammation and histiocyte presence typical of a normal wound healing response were observed at all time points. Allograft adipose matrix maintained form and was visible at week 24 grossly and histologically. Depending on the concentration at which the allograft adipose matrix was reconstituted, the percentage of material retained at week 24 was 44 ± 16 percent (n = 26 replicates).

Masson trichrome staining showed cellular infiltration by week 3, and blood vessels were present within the graft interior. [**See Figure, Supplemental Digital Content 5**, which shows the histologic analysis of acellular adipose matrix implanted into immunocompromised mice, showing the presence of adipocytes within the material. *Scale bar* = 1000 μm for all images. (*Left*) Masson trichrome staining was performed to assess implant architecture and reveal adipocytes present at 3 weeks, with increasing frequency to 24 weeks. (*Right*) Immunohistochemistry with antibodies against perilipin A revealed positive expression of unilocular cells at 3 weeks and increased presence in the graft at each time point until 24 weeks. *Scale bars* = 100 μm. The intended purpose was to provide a broader Masson trichrome and perilipin A imagery time course, expanding on data shown in Fig. 2, ***http://links.lww.com/PRS/D244***.] At early time points, infiltration with fibrocytes and fibroblasts that were most dense within 200 μm of the graft periphery were observed. Neutrophils and macrophages were also abundant at week 3. At week 6, active phagocytic macrophages with eosinophilic debris were evident throughout. At consecutive 12-, 18-, and 24-week time points, the density of macrophages decreased. Perilipin-positive adipocytes were evident within the allograft adipose matrix at week 3 in close proximity to blood vessels (**See Figure, Supplemental Digital Content 5**, *left, yellow arrows*, http://links.lww.com/PRS/D244), and the density of perilipin-expressing adipocytes increased at every subsequent time point (**See Figure, Supplemental Digital Content 5**, *left*, ***http://links.lww.com/PRS/D244***).

Clinical Outcomes and Presurgical and Postsurgical Imaging

All patients received an allograft adipose matrix injection in the dorsal wrist and were monitored for 16 weeks. Follow-up suggested continual integration of the biocompatible graft, safe for subcutaneous injection. Patients (n = 15) were injected by two investigators at separate clinical locations, New York (n = 8) and Florida (n = 7), with average volumes of 4.4 ± 0.6 cc for New York and 3.3 ± 1.4 cc for Florida. Injected volumes between investigators were not statistically different (p = 0.082). Although 15 patients were enrolled in the study, results from 14 patients are included here, as one patient was not present for all evaluations. Patients underwent photography on injection and again at all follow-up time points, 2, 10, and 16 weeks after injection. At week 0, images before and after injection were taken for comparison. Wrist images were taken at the zero-degree position from the radial and ulnar perspectives. Selected images from the time course are presented in Figure 3. Representative images from the intermediate time points—weeks 2 and 10—are shown. [**See Figure, Supplemental Digital Content 6**, which shows selected representative images of the dorsal wrist in the radial (*left*) and ulnar (*right*) views in one representative patient at each time point of the clinical investigation. In the images obtained immediately after injection, the *orange markings* outline the 1 × 5-cm injection site; the hand in these images also displays postinjection swelling, which was common among the patients. The intended purpose was to provide a broader dorsal wrist imagery time course, expanding on data shown (Fig. 3), inclusive of the intermediate time points, ***http://links.lww.com/PRS/D245***.] Patients were asked to report major and/or minor observations or occurrences. No major occurrences, which were defined as infection, allergic reaction, and/or immune response, were observed. Minor observations included wrist pain (n = 15), injection-site redness (n = 13), injection-site swelling (n = 9), itching (n = 5), and wrist tenderness (n = 3). All minor occurrences resolved by the 2-week follow-up except for some continued minor pain (n = 3), which resolved by week 8. In addition, some migration of the material from the injection space was noted (n = 3). A scoring system was implemented, and during follow-up, physicians qualitatively assessed volume retention on a scale of 5 to −1, where 5 denoted the benchmark injection volume, 0 denoted no volume retained, and −1 denoted suspected tissue atrophy. These values were loosely correlated to percentage-based retention values proportionally scaled from 100 percent (denoted by 5) to visible tissue atrophy being described as −20 percent (denoted by −1). (**See Table, Supplemental Digital Content 7**, which shows normalization and scoring system used to grade the volume retention of allograft

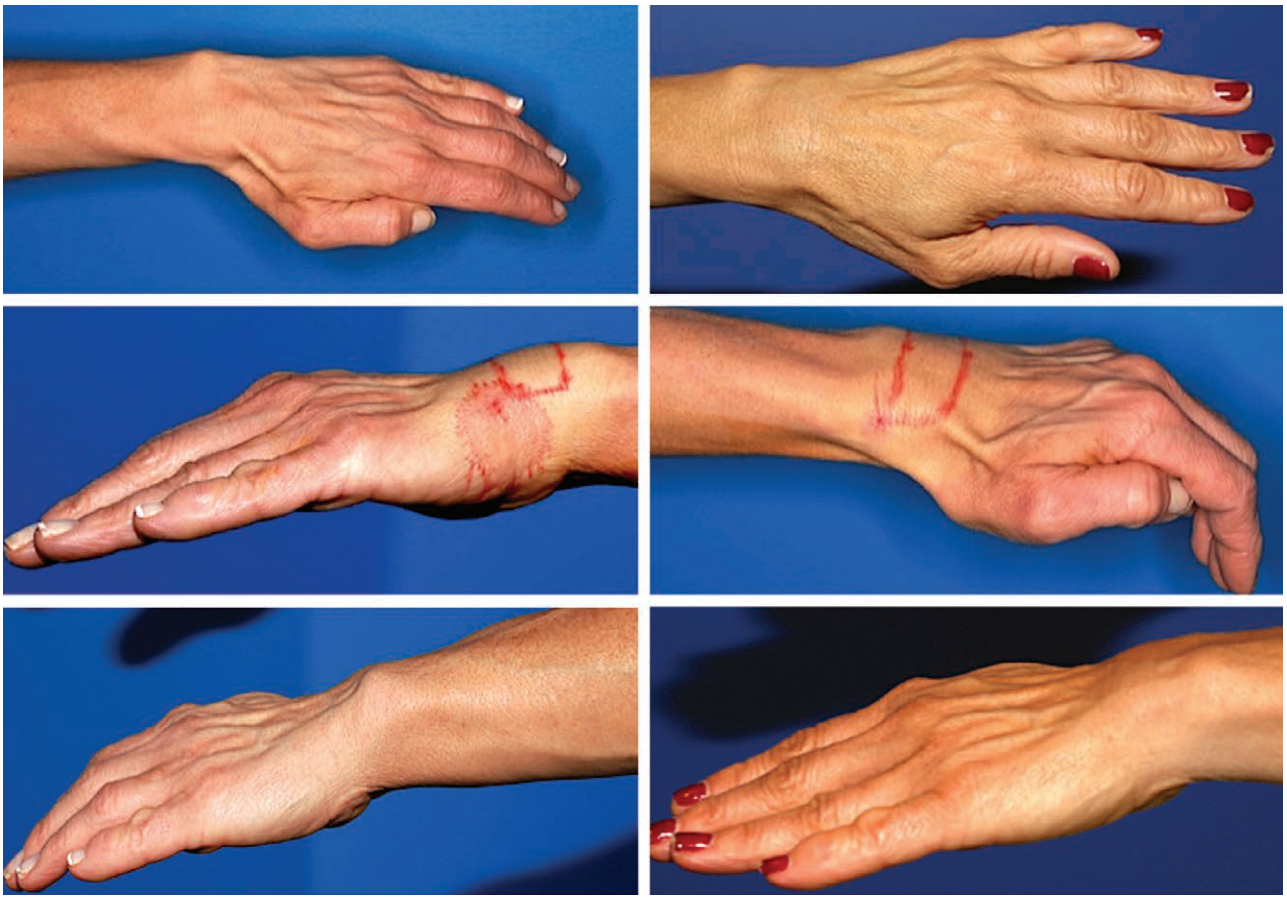

Fig. 3. Selected representative images of the dorsal wrist are shown in the radial and ulnar views in one representative patient. In the images obtained immediately after injection, the *orange markings* outline the 1 × 5-cm injection site; the hand in these images also displays postinjection swelling, which was common among the patients.

adipose matrix throughout the duration of the clinical investigation. The intended purpose was to provide the scoring systems used for grading the allograft adipose matrix retention throughout the clinical investigation, ***http://links.lww.com/PRS/D246***.) Individual patient scores at each time point are presented, along with patient weight and injection volume. (**See Table, Supplemental Digital Content 8**, which shows patient data from clinical investigation, including physician-ranked volume retention at each follow-up; 14 of 15 patients' data are shown, as one patient was not present for follow-up at weeks 10 and 16 and was therefore excluded. The intended purpose was to provide the entire data set of allograft adipose matrix retention scores across all time points, clinical sites, and patients. *ID*, identification; *AAM*, allograft adipose matrix, ***http://links.lww.com/PRS/D247***.)

The average graft retention at 16 weeks was correlated as approximately 47 percent relative to the initial injection volume (average injection volume, 3.9 ± 1.2 cc). A correlation was observed between the injected volume and the retained volume (Fig. 4, *above*). For injections of 4 cc or less, there was significantly less volume retained (approximately 25 percent) compared to patients injected with 4.5 cc or more (approximately 77 percent), shown in Figure 4, *below* ($p = 0.012$). Clinically, it was observed that the prominence of veins and tendons of the dorsal wrist were diminished after injection, and all patients presented apparent thickening and enhancement of quality of the skin through the time course. Histologic evaluation of a biopsy specimen from 16 months after injection indicated that no inflammation or necrosis was present. This segment also contained an area of hemorrhage likely caused by the biopsy (Fig. 5, *left*). In another tissue segment, a small number of perilipin A–positive adipocytes were present adjacent to skin adnexa. Perilipin A–positive staining confirmed a segment containing several clusters of adipose tissue (Fig. 5, *right*).

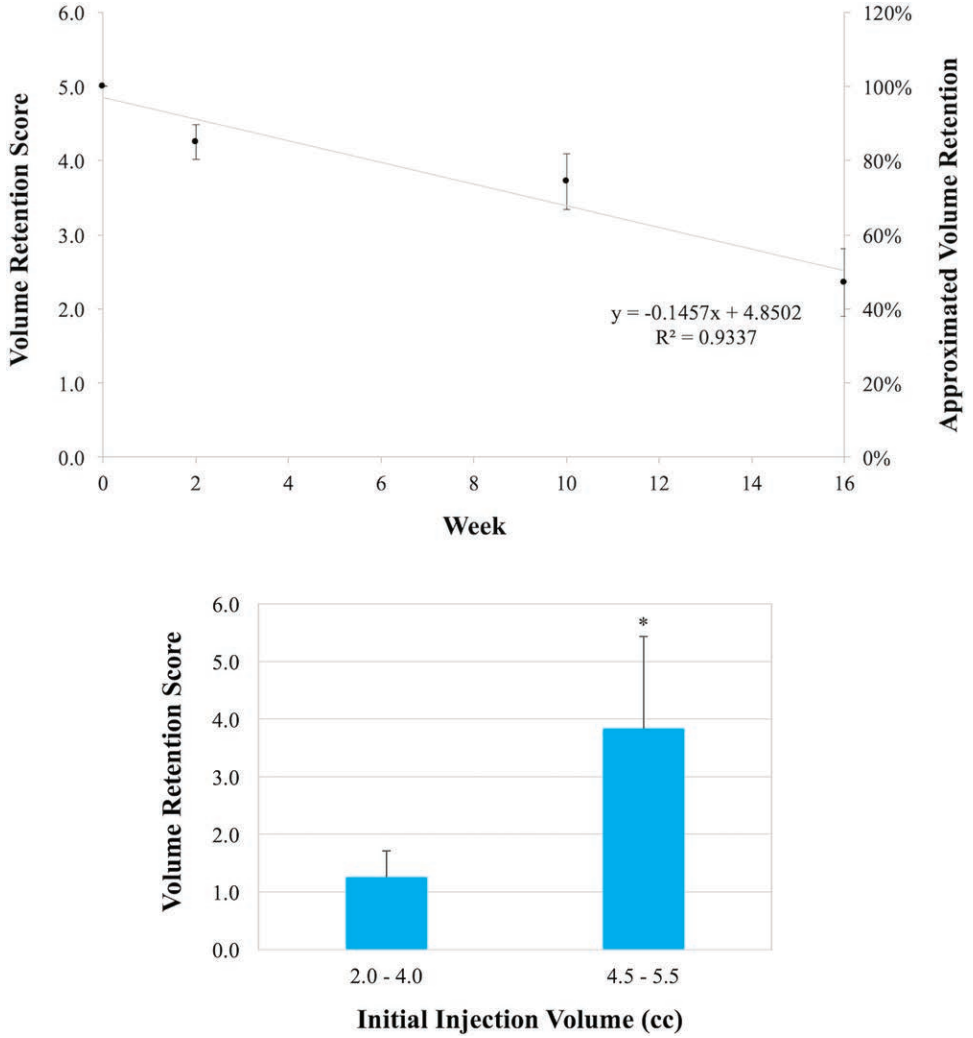

Fig. 4. Descriptive statistics regarding the volume retention in the patient population injected with allograft adipose matrix. (*Above*) The plot displays the compiled data from 14 patients regarding the approximated allograft adipose matrix volume retention at the time of follow-up. Standard error bars are shown. (*Below*) Two-way *t* test shows that approximately twice the volume is retained when larger injection volumes are administered after normalization ($p = 0.012$).

DISCUSSION

Aseptically processed allograft adipose matrix from donated human tissue has been shown to possess angiogenic and adipogenic potential for remodeling and regenerating subcutaneous soft tissue through in vitro cell-matrix studies, in vivo implantation in a preclinical murine model, and preliminary clinical evaluation. Allograft adipose matrix without medium-based stimulus demonstrates human adipose-derived stem cell differentiation into adipocytes through cell morphology, secretion of adipogenic matrix proteins, and lipid accumulation. Adipogenic properties of allograft adipose matrix are also supported by the presence of host adipocytes in subcutaneously injected allograft adipose matrix in the dorsum of athymic mice as early as week 3 after injection. These results are corroborated by qualitative volumetric retention data from 14 patients assessed by two physicians, and histologic evidence of adipocytes in a biopsy specimen from one injected wrist.

The observed adipogenic properties of allograft adipose matrix are attributable at least in part to structural proteins and endogenous adipogenic and angiogenic factors associated with the extracellular matrix, which are preserved through aseptic processing. Type IV and type VI collagen are retained in allograft adipose matrix, and may provide a structural framework for adipose tissue formation. A variety of growth factors are shown to be within allograft adipose matrix, including vascular endothelial growth factor,[24]

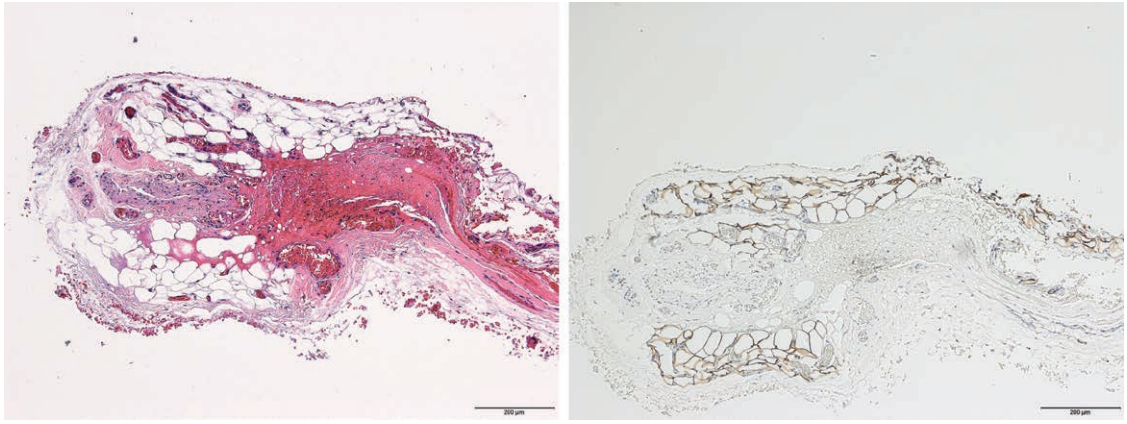

Fig. 5. Histopathologic commentary from patient at 16 months after injection of allograft adipose matrix. (*Left*) Neither inflammation nor necrosis was present. (*Right*) Tissue fragment containing several clusters of perilipin A adipose tissue is adjacent to dilated vasculature.

acidic fibroblast growth factor,[25,26] basic fibroblast growth factor-2,[27–29] insulin-like growth factor-1, and bone morphogenetic protein-9.[30,31] Advantageously, tissue necrosis factor-α, a proinflammatory adipokine up-regulated in obesity,[32] is shown to be removed by the allograft adipose matrix process. Although transforming growth factor-β has been linked to inhibition of adipogenesis, it is essential for matrix formation in adipose tissue.[33] These growth factors have been shown to be retained in allograft adipose matrix, supporting the hypothesis that allograft adipose matrix itself is inherently adipogenic.

The adipogenic nature of allograft adipose matrix is demonstrated through in vitro cell studies. Human adipose-derived stem cells cultured on allograft adipose matrix interacted with allograft adipose matrix, leading to cell attachment, proliferation, and differentiation along with extensive matrix deposition. A major characteristic of adipogenesis is cell shape transformation, as the adipocyte-bound cell changes morphology from fibroblastic to spherical.[34] Scanning electron microscopy and confocal imaging was performed to observe the cell morphology and cell–allograft adipose matrix interactions, showing that human adipose-derived stem cell integrated with allograft adipose matrix three-dimensionally. The newly synthesized extracellular matrix observed surrounding the rounded cells suggested adhesion and integration of the cells within allograft adipose matrix. Histologic analysis demonstrated that the human adipose-derived stem cells took on adipocyte morphology, underwent lipogenesis, and expressed prominent adipogenic markers, including adiponectin,[35] FABP4,[36] and leptin,[37] signifying the differentiation process of adipose-derived stem cells into adipocytes.[38] Histologic analysis further demonstrated the ability of allograft adipose matrix to promote the deposition of basement membrane components, laminin and collagen IV, and collagen VI, known to aid in graft incorporation and long-term remodeling.[18] Human adipose-derived stem cells seeded onto allograft adipose matrix in the absence of adipogenic media stimuli underwent adipogenesis, demonstrating that allograft adipose matrix retained inherent adipogenic cues that support human adipose-derived stem cell attachment, proliferation, and differentiation.

The natural adipogenic activity of allograft adipose matrix was further supported in the in vivo murine transplantation study, where perilipin-positive adipocytes were present in the injected matrix as early as week 3 after injection and increased in numbers throughout the investigation until the final time point at week 24. It was observed that allograft adipose matrix was initially infiltrated with macrophages that decreased in frequency with a corresponding increase in adipocyte concentration, which is consistent with other published studies.[39,40] Previous research in adipose tissue engineering has shown that macrophages are critical for the formation and maintenance of adipose tissue, perhaps because macrophages promote angiogenesis.[41]

Despite the success of autologous fat grafting for volumetric replacement and contouring in aesthetic and reconstructive applications, the procedure is not without its challenges, particularly in the lipodystrophic patient population that cannot sufficiently supply adipose tissue for

transplantation. In the pilot clinical assessment, patients received allograft adipose matrix injections in the range of 2.5 to 5.5 cc into a 1 × 5-cm subcutaneous space of the dorsum of the nondominant wrist. Biocompatibility, volume retention, and soft-tissue rejuvenation were evaluated over a 16-week period. Graft-related redness, pain/soreness, swelling, and/or itching were demonstrated in patients between the time of injection and the first follow-up at week 2. This was most likely caused by the initial inflammation, which can be seen in the images obtained immediately after injection (Fig. 3), and the remodeling phase corroborated by the histologic results seen in the athymic mice (**see Figure, Supplemental Digital Content 5, *http://links.lww.com/PRS/D244***). As shown in the wrist images and the semiquantitative assessment (Fig. 4, *above*), volume retention and skin thickening can be seen through the week-16 follow-up. Although the source of volume retention cannot be definitively concluded, it is hypothesized that graft remodeling may have promoted an adipogenic cascade, leading to observed volume retention. This hypothesis is corroborated by the histologic outcomes from the athymic mice at the 12-, 18-, and 24-week time points. Histologic analysis of a biopsy specimen from the clinical wrist study also showcases disparate adipocyte clusters near large vasculature accesses, supporting the hypothesis of de novo adipogenesis prompted by the injected material as the mechanism of volume retention in the patient. It should be noted that the biopsy specimen for histologic evaluation was obtained 16 months after injection, and evaluation of this kind was limited to an individual patient. Additional clinical limitations in this investigation include the total number of patients enrolled in the study, and, because this investigation marked the first clinical use of allograft adipose matrix, a range of 2.5 to 5.5 cc was injected. This range of injection volume may have led to inconsistencies in graft retention, as suggested in the volumetric analysis in Figure 4, *below*.

Insufficiencies remain in understanding how allograft adipose matrix proteins interact with infiltrating host cells. Although soluble factors and membrane proteins were confirmed, their effects at each stage of the angiogenic and adipogenic cascades were not fully appreciated here. In addition, the injection-site microenvironment may be deterministic to cells infiltrating the graft, as it is populated by neighboring host tissues; because the subcutaneous spaces in the athymic mouse flank and the human dorsal wrist are limited in adipose depots, application of allograft adipose matrix into areas of higher adipose tissue content may better favor adipogenesis. Finally, the use of the athymic mouse model in this investigation may limit preclinical to clinical translation in terms of mechanisms of action, particularly if the immunogenic response plays some key role in cellular transdifferentiation from the immunomodulatory to the adipogenic pathway.

CONCLUSIONS

A structural human allograft adipose scaffold with retained endogenous proteins has been developed for applications in adipose tissue regeneration. Results from cell-matrix interactions in vitro provide evidence that the scaffold is adipoinductive when seeded with human adipose-derived stem cells. This observation is supported by histologic analyses demonstrating adipose depots in athymic mice after 24 weeks inhabiting the implantation site originally occupied by the injected allograft adipose matrix. These preclinical data support the clinical findings of sustained volume retention over 16 weeks on injection of allograft adipose matrix into the dorsal wrist, which is further corroborated by a 16-month biopsy and histologic investigation presenting perilipin-positive adipocytes residing in the allograft adipose matrix injection space.

J. Peter Rubin, M.D.
Department of Plastic Surgery
School of Medicine
University of Pittsburgh
3550 Terrace Street
Pittsburgh, Pa. 15213
rubipj@upmc.edu

REFERENCES

1. Humble G, Mest D. Soft tissue augmentation using Sculptra. *Facial Plast Surg.* 2004;20:157–163.
2. Cox SE, Adigun CG. Complications of injectable fillers and neurotoxins. *Dermatol Ther.* 2011;24:524–536.
3. Fisher C, Grahovac TL, Schafer ME, Shippert RD, Marra KG, Rubin JP. Comparison of harvest and processing techniques for fat grafting and adipose stem cell isolation. *Plast Reconstr Surg.* 2013;132:351–361.
4. Kølle SF, Fischer-Nielsen A, Mathiasen AB, et al. Enrichment of autologous fat grafts with ex-vivo expanded adipose tissue-derived stem cells for graft survival: A randomised placebo-controlled trial. *Lancet* 2013;382:1113–1120.
5. Reing JE, Brown BN, Daly KA, et al. The effects of processing methods upon mechanical and biologic properties of porcine dermal extracellular matrix scaffolds. *Biomaterials* 2010;31:8626–8633.
6. Sicari BM, Rubin JP, Dearth CL, et al. An acellular biologic scaffold promotes skeletal muscle formation in mice and humans with volumetric muscle loss. *Sci Transl Med.* 2014;6:234ra58.

7. Shepherd N, Greenwell H, Hill M, Vidal R, Scheetz JP. Root coverage using acellular dermal matrix and comparing a coronally positioned tunnel with and without platelet-rich plasma: A pilot study in humans. *J Periodontol.* 2009;80:397–404.
8. Brown AL, Brook-Allred TT, Waddell JE, et al. Bladder acellular matrix as a substrate for studying in vitro bladder smooth muscle-urothelial cell interactions. *Biomaterials* 2005;26:529–543.
9. Reddy PP, Barrieras DJ, Wilson G, et al. Regeneration of functional bladder substitutes using large segment acellular matrix allografts in a porcine model. *J Urol.* 2000;164:936–941.
10. Zhang X, Yang J, Li Y, et al. Functional neovascularization in tissue engineering with porcine acellular dermal matrix and human umbilical vein endothelial cells. *Tissue Eng Part C Methods* 2011;17:423–433.
11. Wu I, Nahas Z, Kimmerling KA, Rosson GD, Elisseeff JH. An injectable adipose matrix for soft-tissue reconstruction. *Plast Reconstr Surg.* 2012;129:1247–1257.
12. Choi JS, Yang HJ, Kim BS, et al. Human extracellular matrix (ECM) powders for injectable cell delivery and adipose tissue engineering. *J Control Release* 2009;139:2–7.
13. Han TT, Toutounji S, Amsden BG, Flynn LE. Adipose-derived stromal cells mediate in vivo adipogenesis, angiogenesis and inflammation in decellularized adipose tissue bioscaffolds. *Biomaterials* 2015;72:125–137.
14. Flynn LE. The use of decellularized adipose tissue to provide an inductive microenvironment for the adipogenic differentiation of human adipose-derived stem cells. *Biomaterials* 2010;31:4715–4724.
15. Choi JS, Kim BS, Kim JY, et al. Decellularized extracellular matrix derived from human adipose tissue as a potential scaffold for allograft tissue engineering. *J Biomed Mater Res A* 2011;97:292–299.
16. Brown BN, Freund JM, Han L, et al. Comparison of three methods for the derivation of a biologic scaffold composed of adipose tissue extracellular matrix. *Tissue Eng Part C Methods* 2011;17:411–421.
17. Sano H, Orbay H, Terashi H, Hyakusoku H, Ogawa R. Acellular adipose matrix as a natural scaffold for tissue engineering. *J Plast Reconstr Aesthet Surg.* 2014;67:99–106.
18. Mariman EC, Wang P. Adipocyte extracellular matrix composition, dynamics and role in obesity. *Cell Mol Life Sci.* 2010;67:1277–1292.
19. Patrick CW, Uthamanthil R, Beahm E, Frye C. Animal models for adipose tissue engineering. *Tissue Eng Part B Rev.* 2008;14:167–178.
20. Ullmann Y, Hyams M, Ramon Y, Beach D, Peled IJ, Lindenbaum ES. Enhancing the survival of aspirated human fat injected into nude mice. *Plast Reconstr Surg.* 1998;101:1940–1944.
21. Shoshani O, Ullmann Y, Shupak A, et al. The role of frozen storage in preserving adipose tissue obtained by suction-assisted lipectomy for repeated fat injection procedures. *Dermatol Surg.* 2001;27:645–647.
22. Ramon Y, Shoshani O, Peled IJ, et al. Enhancing the take of injected adipose tissue by a simple method for concentrating fat cells. *Plast Reconstr Surg.* 2005;115:197–201; discussion 202–203.
23. Chung CW, Marra KG, Li H, et al. VEGF microsphere technology to enhance vascularization in fat grafting. *Ann Plast Surg.* 2012;69:213–219.
24. Song SY, Chung HM, Sung JH. The pivotal role of VEGF in adipose-derived-stem-cell-mediated regeneration. *Expert Opin Biol Ther.* 2010;10:1529–1537.
25. Hutley L, Shurety W, Newell F, et al. Fibroblast growth factor 1: A key regulator of human adipogenesis. *Diabetes* 2004;53:3097–3106.
26. Widberg CH, Newell FS, Bachmann AW, et al. Fibroblast growth factor receptor 1 is a key regulator of early adipogenic events in human preadipocytes. *Am J Physiol Endocrinol Metab.* 2009;296:E121–E131.
27. Kühn MC, Willenberg HS, Schott M, et al. Adipocyte-secreted factors increase osteoblast proliferation and the OPG/RANKL ratio to influence osteoclast formation. *Mol Cell Endocrinol.* 2012;349:180–188.
28. Berti L, Irmler M, Zdichavsky M, et al. Fibroblast growth factor 21 is elevated in metabolically unhealthy obesity and affects lipid deposition, adipogenesis, and adipokine secretion of human abdominal subcutaneous adipocytes. *Mol Metab.* 2015;4:519–527.
29. Kim S, Ahn C, Bong N, Choe S, Lee DK. Biphasic effects of FGF2 on adipogenesis. *PLoS One* 2015;10:e0120073.
30. Song D, Zhang F, Reid RR, et al. BMP9 induces osteogenesis and adipogenesis in the immortalized human cranial suture progenitors from the patent sutures of craniosynostosis patients, *J Cell Mol Med.* 2017;21:2782–2795.
31. Garten A, Schuster S, Kiess W. The insulin-like growth factors in adipogenesis and obesity. *Endocrinol Metab Clin North Am.* 2012;41:283–295, v.
32. Coppack SW. Pro-inflammatory cytokines and adipose tissue. *Proc Nutr Soc.* 2001;60:349–356.
33. Choy L, Derynck R. Transforming growth factor-beta inhibits adipocyte differentiation by Smad3 interacting with CCAAT/enhancer-binding protein (C/EBP) and repressing C/EBP transactivation function. *J Biol Chem.* 2003;278:9609–9619.
34. Qian SW, Li X, Zhang YY, et al. Characterization of adipocyte differentiation from human mesenchymal stem cells in bone marrow. *BMC Dev Biol.* 2010;10:47.
35. Sowers JR. Endocrine functions of adipose tissue: Focus on adiponectin. *Clin Cornerstone* 2008;9:32–38; discussion 39–40.
36. Furuhashi M, Saitoh S, Shimamoto K, Miura T. Fatty acid-binding protein 4 (FABP4): Pathophysiological insights and potent clinical biomarker of metabolic and cardiovascular diseases. *Clin Med Insights Cardiol.* 2014;8(Suppl 3):23–33.
37. Wauters M, Considine RV, Van Gaal LF. Human leptin: From an adipocyte hormone to an endocrine mediator. *Eur J Endocrinol.* 2000;143:293–311.
38. Satish L, Krill-Burger JM, Gallo PH, et al. Expression analysis of human adipose-derived stem cells during in vitro differentiation to an adipocyte lineage. *BMC Med Genomics* 2015;8:41–52.
39. Li Z, Xu F, Wang Z, et al. Macrophages undergo M1-to-M2 transition in adipose tissue regeneration in a rat tissue engineering model. *Artif Organs* 2016;40:E167–E178.
40. Valentin JE, Stewart-Akers AM, Gilbert TW, Badylak SF. Macrophage participation in the degradation and remodeling of extracellular matrix scaffolds. *Tissue Eng Part A* 2009;15:1687–1694.
41. Debels H, Galea L, Han XL, et al. Macrophages play a key role in angiogenesis and adipogenesis in a mouse tissue engineering model. *Tissue Eng Part A* 2013;19:2615–2625.